Structural changes in GroEL effected by binding a denatured protein substrate

ARTICLE *in* JOURNAL OF MOLECULAR BIOLOGY · JUNE 2001

Impact Factor: 4.33 · DOI: 10.1006/jmbi.2001.4613 · Source: PubMed

3 AUTHORS, INCLUDING:

Mark T Fisher
University of Kansas
58 PUBLICATIONS **1,206** CITATIONS
SEE PROFILE

Edward P Gogol
University of Missouri - Kansas City
41 PUBLICATIONS **1,556** CITATIONS
SEE PROFILE

doi:10.1006/jmbi.2001.4613 available online at http://www.idealibrary.com on IDEAL® J. Mol. Biol. (2001) 308, 569–577

JMB

COMMUNICATION

Structural Changes in GroEL Effected by Binding a Denatured Protein Substrate

Scott Falke[1], Mark T. Fisher[1] and Edward P. Gogol[2]*

[1]*Department of Biochemistry and Molecular Biology, University of Kansas Medical Center, Kansas City KS 66160, USA*

[2]*School of Biological Sciences University of Missouri-Kansas City, Kansas City MO 64110, USA*

**Corresponding author*

In the absence of nucleotides or cofactors, the *Escherichia coli* chaperonin GroEL binds select proteins in non-native conformations, such as denatured glutamine synthetase (GS) monomers, preventing their aggregation and spontaneous renaturation. The nature of the GroEL-GS complexes thus formed, specifically the effect on the conformation of the GroEL tetradecamer, has been examined by electron microscopy. We find that specimens of GroEL-GS are visibly heterogeneous, due to incomplete loading of GroEL with GS. Images contain particles indistinguishable from GroEL alone, and also those with consistent identifiable differences. Side-views of the modified particles reveal additional protein density at one end of the GroEL-GS complex, and end-views display chirality in the heptameric projection not seen in the unliganded GroEL. The coordinate appearance of these two projection differences suggests that binding of GS, as representative of a class of protein substrates, induces or stabilizes a conformation of GroEL that differs from the unliganded chaperonin. Three-dimensional reconstruction of the GroEL-GS complex reveals the location of the bound protein substrate, as well as complex conformational changes in GroEL itself, both *cis* and *trans* with respect to the bound GS. The most apparent structural alterations are inward movements of the apical domains of both GroEL heptamers, protrusion of the substrate protein from the cavity of the *cis* ring, and a narrowing of the unoccupied opening of the *trans* ring.

Keywords: GroEL; chaperonin; electron microscopy; protein folding

The GroE proteins of *Escherichia coli* comprise the essential two-component chaperonin system required for the ATP-dependent folding of many newly synthesized proteins, under both normal and stress-induced conditions. The larger of the two components, GroEL, is a 57 kDa protein that assembles into a complex made up of two toroidal GroEL heptamers (Braig *et al*., 1994; Roseman *et al*., 1996). The GroEL monomer is composed of two large domains, equatorial and apical, located at the center and ends of the tetradecameric complex, respectively, linked by a third, smaller, intermediate domain. The equatorial domains contain nucleotide-binding sites, and are the regions of interaction between the two GroEL heptamers. The apical domains of each GroEL heptamer define a central cavity lined with hydrophobic residues that various lines of evidence suggest as the initial binding site for newly synthesized or misfolded polypeptides (Braig *et al*., 1994; Fenton *et al*., 1994). The intermediate domain linking the apical and equatorial domains provides flexibility for rearrangements of the two larger domains in response to the binding of nucleotides and the co-chaperonin, GroES.

The smaller component of the chaperonin system, GroES, is a 10 kDa protein that assembles into heptamers, forming a cap-like structure that interacts with either end of the cylindrical GroEL assembly (Hunt *et al*., 1996; Mande *et al*., 1996). Its nucleotide-dependent interaction with GroEL induces a large structural rearrangement of the GroEL apical domains, described principally as en bloc rotations of the apical domains, as well as smaller-scale but functionally important changes in the interactions between the intermediate and

Abbreviations used: GS, glutamine synthetase; SANS, small-angle neutron scattering; cryoEM, cryo-electron microscopy.

E-mail address of the corresponding author: gogole@umkc.edu

0022-2836/01/040569–9 $35.00/0

equatorial domains (Roseman *et al*., 1996; Xu *et al*., 1997). The net effect of the major rearrangement is an expansion of the GroEL cavity (from ~85,000 Å^3 to ~175,000 Å^3), along with burial of the previously exposed hydrophobic residues lining it, thereby changing the nature of the interaction of the chaperonin with substrate polypeptides. The size of the unexpanded cavity is estimated to be sufficient to contain an unfolded protein of up to ~35 kDa, or a native one of about twice that size (Xu *et al*., 1997). Refolding studies on a series of protein concatamers have supported this estimated capacity of the GroEL cavity (Sakikawa *et al*., 1999).

Extensive biochemical studies of the GroE activity cycle have elucidated a possible pathway of assisted protein folding, and structural analyses by crystallography and electron microscopy have provided some of the mechanistic details of the process (reviewed by Sigler *et al*. (1998) and Rye *et al*., 1999). Characterization of the cooperativity in nucleotide binding within each GroEL heptamer, and anti-cooperativity between heptamers in both nucleotide and GroES binding (Yifrach & Horovitz, 1995, 1996), has provided important clues to the mechanism of facilitated binding and release of substrate proteins. Three-dimensional reconstruction of electron microscopic images has identified configurations of GroEL correlated with the nature of bound nucleotide (Roseman *et al*., 1996; White *et al*., 1997), giving a direct structural component to a model dependent on the hydrolysis of ATP. The current paradigm of the GroEL cycle, based on a combination of structural and functional studies, is that of a molecular machine that alternates between high and low affinity states for non-native polypeptides, controlled by the consecutive binding of ATP and GroES to each half of the GroEL complex (Fenton & Horwich, 1997; Xu & Sigler, 1998).

Biochemical studies have suggested that polypeptide substrates may influence the structure of GroEL, at least in the presence of nucleotide and GroES (Churchich, 1997; Mendoza & Campo, 1996). Although complexes of GroEL with small (<40 kDa) substrate proteins have been studied by electron microscopy and small-angle neutron scattering (SANS), conformational changes in GroEL consistent with biochemical studies have not been documented (Chen *et al*., 1994; Thiyagarajan *et al*., 1996). The lack of observable structural alterations suggests that changes induced by small substrates may be too limited to be apparent by electron microscopy or SANS, or that nucleotide and/or GroES are required to effect a conformational change. Addressing these questions may require examination of a complex of GroEL, in the absence of other cofactors, with a substrate protein possessing the appropriate properties (e.g. a size above ~40 kDa) that may induce a clearly observable structural correlate to the biochemically detected alterations.

Both elements of the GroE system (EL and ES) are available and presumably used for *in vivo* protein folding. However, *in vitro* experiments have demonstrated the ability of GroEL and ATP to promote the renaturation of some, but not all, proteins, with yields comparable to those achieved with the complete chaperonin system (Coyle *et al*., 1999; Schmidt *et al*., 1994). Examination of the variation in the stringency of requirement for GroES, or for ATP hydrolysis, may reveal variations in mechanism or overall pathway employed by the GroE system (Wang & Weissman, 1999). A well-studied example of GroEL-mediated protein refolding in the absence of GroES is the renaturation of chemically denatured *E. coli* glutamine synthetase (GS) monomers, and their subsequent association into active oligomers (Fisher, 1992). In the absence of additional cofactors (nucleotide or GroES), and over a limited concentration range of protein, GroEL can bind chemically denatured GS and prevent both its aggregation and its spontaneous renaturation. Subsequent addition of ATP under defined conditions yields approximately full reactivation of GS, similar to the levels obtained with the entire GroEL-GroES-ATP system, though with somewhat slower kinetics (Fisher, 1994; Voziyan & Fisher, 2000). Due to its relatively large size (52 kDa), the denatured GS monomer is not expected to be able to bind totally within the crystallographically defined GroEL cavity. We have examined complexes of GroEL with urea-denatured GS by electron microscopy, in the absence of nucleotide, to describe the structural ramifications of this association.

Our preparative goal in this structural study was to load denatured GS onto GroEL to maximum capacity (up to one GS monomer per GroEL tetradecamer) to minimize heterogeneity in the data set, thereby reducing the complexity of subsequent image analysis. At concentrations above ~0.4 μM, denatured GS kinetically partitions into insoluble aggregates upon dilution, rather than binding to GroEL (Fisher, 1993), thus making preparation of specimens of ~1 μM GroEL-GS problematic. To maximize the formation of GroEL-GS complexes, we have used an iterative loading protocol in which small aliquots (~1 μl) of 20 μM GS in 8 M urea (fully denatured by incubation for four hours) were added to 100 μl of 1 μM GroEL in buffer (50 mM Tris-HCl, 50 mM KCl, 10 mM $MgCl_2$, 1 mM DTT, 1 mM EDTA (pH 7.0)) at 37 °C with rapid mixing. The total concentration of GS reached ~1 μM, with residual GS activity revealing minimal unbound GS at each addition, and the total urea concentration remained below 0.5 M.

Specimens of GroEL-GS complexes, and of GroEL alone (both with and without 0.5 M urea), were prepared for electron microscopy by both negative staining with uranyl acetate, and by rapid freezing from thin films prepared on a fenestrated carbon film, in a chamber maintained near 37 °C at near 100 % humidity. Minimal-dose electron micrographs from both types of specimens were

recorded with a JEOL 1200 EX electron microscope, using a Gatan 626-Twin cold stage for cryo-electron microscopy (cryoEM).

Binding of GS to GroEL was analyzed indirectly by measuring the extent of regain of GS enzymatic activity upon addition of ATP, and more directly by native gel electrophoresis (Fisher, 1994). ATP-dependent renaturation of urea-denatured GS by a twofold or higher excess of GroEL, under the conditions used (the buffer described above, two hours at 37 °C), can recover up to ~85 % of the initial GS activity (Fisher, 1993). It is unclear how much of the unrecoverable loss is due to incomplete binding to GroEL, and how much to imperfect oligomerization that is required for full enzymatic activity. In our iteratively loaded 1:1 GroEL:GS specimens, we were able to recover, on average, approximately 73 % of the initial GS activity (Figure 1(a)), a quantity that is ~85 % of that obtained with an excess of GroEL. Hence at least 75 %, and perhaps up to 85 %, of the GS seems to be in complex with GroEL by this criterion. A more direct measure of the binding of GS to GroEL is afforded by the electrophoretic resolution and quantification of the liganded and unliganded GroEL. As illustrated in Figure 1(b), the slower-moving GroEL-GS band accounts for only 40 % of the total GroEL in our 1:1 specimens. It should be noted that electrophoresis was carried out at 16 °C, a drop in temperature that is consistent with partial release of protein substrates from GroEL (Brunschier *et al*., 1993; Lin *et al*., 1995; M. Fisher, personal observation). While we attempted to maintain our EM preparations at 37 °C during preparation, for both types of specimens, the difficulty of gauging the effect of evaporative cooling and, in the case of cryoEM specimens the proximity to the freezing solution, makes an accurate estimation of the temperature immediately prior to final immobilization problematic. Furthermore, temperature variation during the preparation of individual specimens introduces another uncertainly. Hence it is unclear which measurement of GroEL-GS complex formation is the more appropriate for our specimens, but both serve to bracket the range of effectiveness of complex formation, between 40 % and 75-85 %.

A representative field of view of a GroEL-GS cryo-specimen is shown in Figure 2. A range of particle orientations is visible, but two are most prominent: heptagonal end-views and rectangular side-views. Similar distributions of views were noted in cryo-specimens of GroEL alone. Negatively stained specimens displayed less variability in orientation, yielding a predominance of end-views when adsorbed to solid carbon substrate immediately following plasma discharge, and more side-views when carbon substrates were allowed to age for ~1 hour. The only difference that was visible, and only barely, between micrographs of GroEL and GroEL-GS complexes was the presence of a variable fraction of side-views that have a slight asymmetry between the two ends of side-views of the GroEL-GS specimens (indicated in Figure 2). All of the side-views of GroEL, and many of those of GroEL-GS, displayed the more symmetrical rectangular appearance expected, based on its crystal structure.

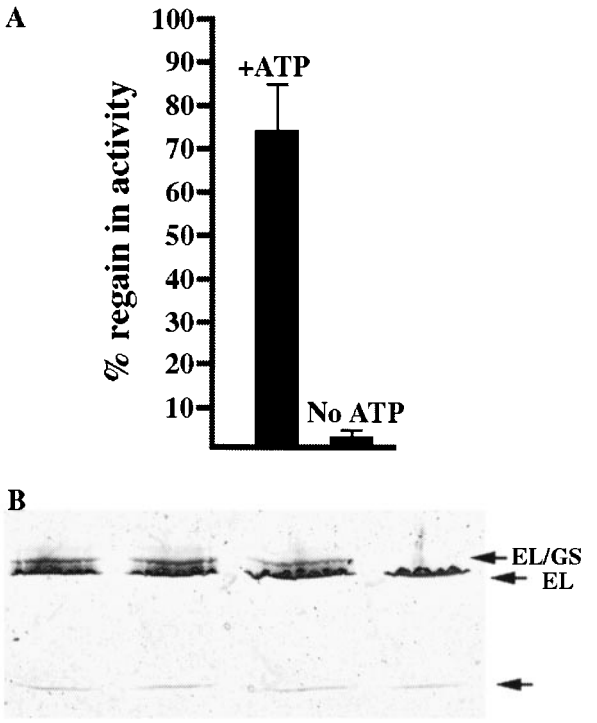

Figure 1. Biochemical characterization of GroEL-GS complexes prepared by the iterative loading procedure described in the text. (a) Recovery of GS activity from GroEL-GS complexes, to a level of ~73(±10) upon addition of ATP, *versus* 3(±2) % in the absence of ATP. GS was denatured in 8 M urea and rapidly diluted 100-fold by addition to a 1 μM solution of GroEL at 37 °C, followed by incubation for two hours ± the addition of 10 mM ATP. (b) Native gel (4-15 % gradient) electrophoresis of GroEL-GS complexes at 1.5:1, 1:1 and 0.5:1 and 0:1 molar ratio of GS to GroEL, from left to right. Positions of GroEL and GroEL-GS complexes are indicated. The faint lower band in each lane (unlabeled arrow) is the small fraction of GroEL heptamer in the GroEL preparation. Quantification of Coomassie-blue-staining intensity using Imagequant (Molecular Dynamics) indicates that the upper band (GroEL-GS complex) represents approximately 43, 40, and 30 %, respectively, of the protein in the three GroEL-GS lanes, from left to right.

To better visualize the observed variation in the GroEL-GS specimens, and to compare with GroEL alone, micrographs of both types of specimens were digitized, aligned, and averaged, using the SPIDER image-analysis programs (Frank *et al*., 1996). Initial averages of side-views, aligned with a reference-independent procedure (Penczek *et al*., 1992), are shown in Figure 3(a), (b), (e) and (f). These averages include various views of the particles rotated about their long axes, and thus are

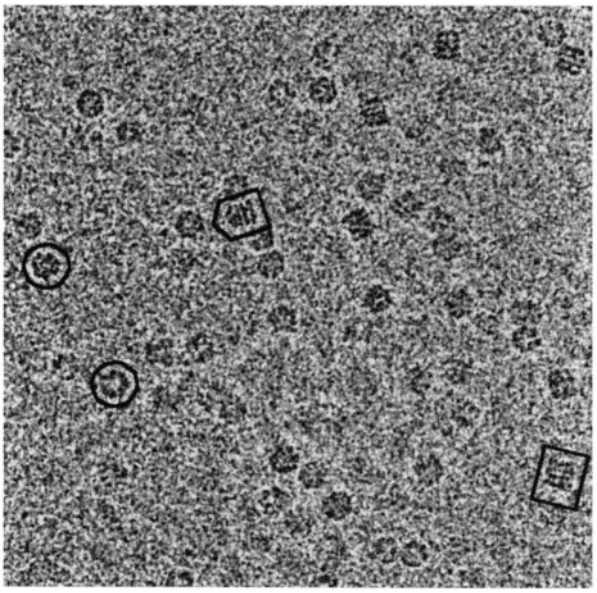

Figure 2. Cryo-electron microscopy field of a GroEL-GS specimen, containing a mixture of orientations of both GroEL and GroEL-GS complexes. Circles identify representative end-views. A 2-fold symmetrical, flat-ended side-view, visually indistinguishable from images of GroEL alone (not shown), is outlined with a rectangle. The particle enclosed in a pentagon exhibits an asymmetry, visible as a bulge or extension at one end, that is not found in preparations of GroEL without GS.

cylindrically averaged projections of the structures; hence only major features (such as the molecular outline) are valid for interpretation. The primary difference between the averages of GroEL and GroEL-GS images, in both negatively stained and cryoEM specimens, is an asymmetry between the two ends of GroEL-GS, in contrast to the more symmetrical GroEL. (All images were aligned to maximize asymmetry.) The bands at either end of the GroEL images ((a) and (e)), representing the projections of the apical domains, have a relatively low density at their centers, due to the opening to the cavity. In contrast, a small but distinct increase in density is present in the center of the right-hand apical bands of the GroEL-GS images ((b) and (f)), presumably a manifestation of the bound GS.

The heterogeneity of the GroEL-GS images was examined by classification of side-view images into two categories using multivariate statistical analysis (correspondence analysis), as implemented in the SPIDER package. Two robust classes of side-views from the GroEL-GS preparations, presumably representing unliganded GroEL and GroEL-GS, were readily identified by hierarchical classification. One of these classes (Figure 3(c) and (g)) resembles the 2-fold symmetrical side-view of GroEL alone, and the other (Figure 3(d) and (h)) exhibits a density in the apical domain region on the right end, larger than that seen in the overall averaged images (Figure 3(b) and (f)). The fraction of particles in the latter category, obtained with both negatively stained and cryoEM specimens, was typically between 50 and 70% of the total. A parallel analysis of images of GroEL in the absence of substrate (not shown) resulted in only unstable classes, none of which exhibited the degree of asymmetry seen in GroEL-GS.

To search for a complementary structural correlate to the differences seen with side-view projections, end-views of GroEL and GroEL-GS were aligned and averaged. Negatively stained GroEL specimens, both with and without GS, revealed the 7-fold symmetry seen in previous electron microscopic analyses (Figure 4(a) and (b)). The major difference between the two specimens was the introduction of chirality in GroEL-GS images, indicating that the 2-fold symmetry of GroEL is disrupted. In addition, the center of the GroEL-GS images consistently excluded stain to a greater extent than unliganded GroEL, indicating either the presence of additional protein density at this location, or a structural change in GroEL, or a combination of the two.

Analysis of the cryoEM end-views presented an alignment problem, possibly due to their lower signal-to-noise ratio. Reference-independent alignment failed to produce clear averages of the particles of either unliganded GroEL or GroEL-GS complexes, when compared to either the negatively stained specimens, or to images aligned to specific references. We overcame this apparent computational limitation by applying 7-fold symmetry to the individual images prior to alignment. Our analysis of the negatively stained end-views indicates that 7-fold symmetry is preserved in the GroEL-GS complexes. Hence symmetrization of the cryoEM images is not likely to compromise significant features. The resulting averaged images (Figure 4(c) and (d)) display the difference in chirality previously seen with our negatively stained specimens. The heterogeneity of GroEL-GS specimens was addressed by separating the images by K-means classification into categories that maximize the overall difference between classes (Penczek *et al.*, 1992). This procedure readily yielded two visibly different categories of GroEL-GS images, one resembling the GroEL average (Figure 4(e)), and the other (Figure 4(f)) a more extreme version of the global average of the GroEL-GS images (Figure 4(d)). The percentage of images falling into the latter class ranged from 40 to 60% of the total, comparable to the results of the analysis of side-views. Attempts to produce larger numbers of classes invariably yielded only additional copies of the two classes shown. When the same K-means classification procedure was attempted with the images of GroEL alone, two (or more) visually similar classes were produced (not shown). Hence we interpret the two visibly different classes of GroEL-GS end-views, in parallel with those of the side-views, as manifestations of GroEL with or without bound GS. The analysis of our cryoEM images supports the interpretation of the

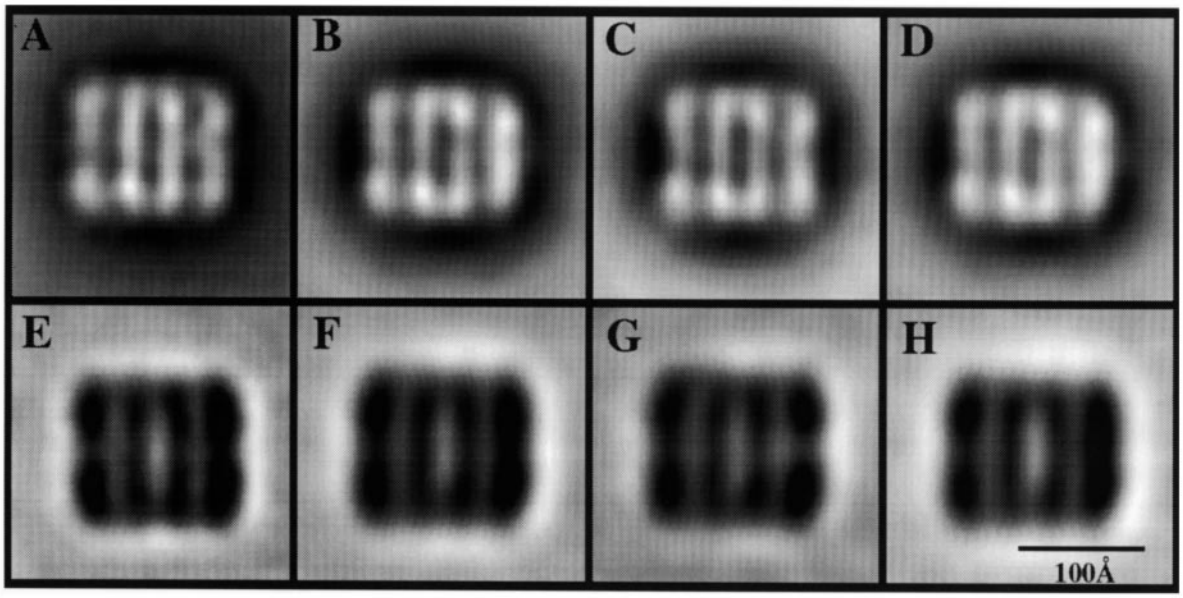

Figure 3. Averaged side-views of negatively stained ((a)-(d)) and cryoEM ((e)-(h)) side-views of GroEL alone (control (a) and (e)) and GroEL-GS ((b) and (f)), aligned to place the higher-density end of each image to the right. The images of the GroEL-GS specimen were sorted by correspondence analysis based on the presence of high density at the right-hand end of the image, producing two well-defined classes, one that appears similar to GroEL alone ((c), (g)) and one that exhibits a distinctly increased and continuous density at its right end ((d), (h)). Parallel attempts at sorting GroEL control ((a) and (e)) failed to identify similar or any other stable classes of images. Number of images in each average: (a) 368; (b) 400; (c) 151; (d) 249; (e) 254; (f) 408; (g) 112; and (h) 296.

difference seen in the negatively stained specimens as a real break from the 2-fold symmetry of GroEL, rather than simply an effect of asymmetric staining or restricted particle orientation caused by binding of GS.

We have explored the possibility that the additional density of denatured GS may cause GroEL to appear structurally asymmetric in end-view projection by modeling its potential effects on projections of the crystal structure. Though reports of other proteins bound to chaperonins indicate that they may bind in an unequal manner to the individual subunits of one ring of the chaperonin (Farr *et al*., 2000; Llorca *et al*., 1999), the analysis of our negatively stained specimens indicates that the GS is not similarly localized. Our models of GroEL-GS distributed the density equivalent to one GS monomer among the seven projected subunits equally, and varied its projected location to maximize its effect on the appearance of the complex. Regardless where the GS density was positioned, effects comparable to those seen in Figure 4(b), (d) and (f) could not be produced, unless a protein mass at least three times that of GS is added to each GroEL. Furthermore, this calculation does not take into account the additional density apparently present at the center of the end-view, which is likely to be a major portion of the GS, and would therefore reduce the effect of the projected density even further. Hence we conclude that the difference in appearance between GroEL and GroEL-GS cannot be accounted for by the additional density of GS alone, but indicates a conformational difference between the GroEL in its unliganded and GS-bound forms.

We have examined the nature of the structural changes effected by the binding of GS to GroEL by three-dimensional analysis: 4998 images of individual particles in random orientations were selected from cryo-electron micrographs of a GroEL-GS specimen, including the side and end-views analyzed in projection. The images were aligned to projections of a model derived from the GroEL crystal structure, calculated in 7.5° steps in angular orientations, representing an evenly spaced set of viewing directions (Euler angles). We dealt with the problem of heterogeneity in GroEL-GS by simultaneously using two models, one of the GroEL alone, and the other modified by addition of a monomer of GS (native structure; Yamashita *et al*., 1989), centered within one of the apical cavities of the chaperonin. No other modification to GroEL was introduced. Each image was aligned to the set of projections from each model, and the best match, determined by maximum correlation coefficient, defined both the preferred model and the Euler angle for that image. Approximately 60% of the images initially aligned best to projections of the unliganded GroEL, with the remainder favoring the GroEL-GS model. Reconstructions were calculated for images corresponding to each model by reciprocal space interpolation and inverse Fourier transformation. The structures were refined for several rounds by using the initial and subsequent reconstructions as new models for *de novo* image alignment and classification. The refinement was

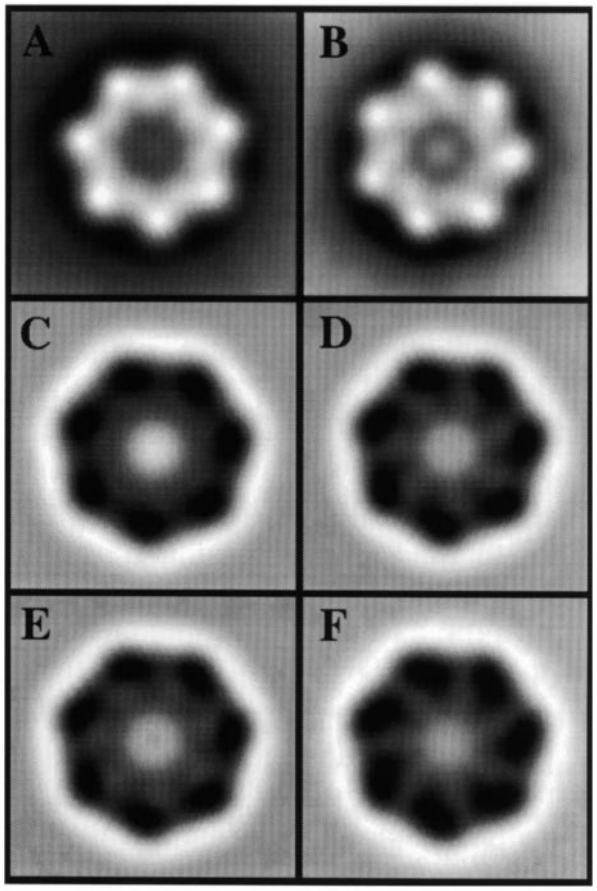

Figure 4. Averaged end-views of negatively stained ((a) and (b)) and cryoEM ((c)-(f)) images of GroEL alone (control, (a) and (c)) and GroEL-GS ((b) and (d)) specimens. All control and GroEL-GS specimens were tested by correlation analysis and mirrored if necessary to standardize their handedness. A difference in the degree of chirality (apparent skewing of the subunits) is visible between control and GroEL-GS averages representing an asymmetric change in the GroEL-GS complex. The heterogeneous GroEL-GS sample was sorted by K-means classification, producing two categories, shown in (e) and (f). Average (e) resembles GroEL alone, and presumably represents GroEL that failed to bind GS. Average (f) exhibits a pronounced difference in projection from GroEL-alone control (c), apparently representing molecules of GroEL complexed with GS. Number of images in each average: (a) 292; (b) 242; (c) 438; (d) 528; (e) 330; and (f) 198.

continued until the number of images changing orientation and model preference reached a minimum (approximately 5% per cycle). In the final stage of refinement, the images were divided between the two reference models by the initial 60:40 ratio.

The three-dimensional reconstructions from the GroEL-GS images are presented in Figure 5 as surface views of both classes. The resolution of each of the final reconstructions is approximately $(26\ \text{Å})^{-1}$, estimated by the reciprocal space shell in which the Fourier ring correlation between reconstructions from two halves of the data reaches a value of 0.5. The phase difference residuals are approximately 55° at this resolution. The structure derived from the first reference (Figure 5(a)-(d)) is consistent with the published crystal and EM structures of GroEL. The most apparent difference in the second reconstruction (that derived from the model that includes a GS monomer) is the presence of a distinct bulge, presumably representing bound GS, at one end of GroEL (Figure 5(f)-(i)). During refinement of the GroEL-GS structure, this density migrated from its initial modeled position fully within the cavity to one of partial apical protrusion. This location is similar to that of the smaller substrates malate dehydrogenase and rhodanese, deduced from cryoEM and SANS, respectively (Chen *et al.*, 1994; Thiyagarajan *et al.*, 1996), and is consistent with the appearance of our side-view averages. Insofar as the structure of the GroEL itself is concerned, the three-dimensional analysis shows differences in both the *cis* and *trans* rings of GroEL-GS in comparison to unliganded GroEL. The most notable changes are movements of the apical domains of both heptamers, including an inward radial repositioning that reduces the diameter of the GroEL at both ends, yielding an appearance that looks slightly tapered at either end. A similar tapering of the apical domains has been observed in side-view projections of negatively stained images of GroEL prepared in the presence of ATP at elevated temperature (Llorca *et al.*, 1998). Details of the apical domains at the two ends, while not clearly resolved in the reconstructions, appear to differ between the *cis* and *trans* rings. This difference is revealed in part by calculating the end-view projection of each reconstruction, shown in Figure 5(e) and (j). While the projection of the GroEL without GS bound shows no sign of chirality, that of the second class of images (with GS bound), exhibits a handedness, specifically at the inner edges of the seven high densities at the periphery of the structure. These features are similar to those noted in the averaged images of GroEL-GS end-views (Figure 4). They differ in intensity and detail, possibly due to the inclusion of a range of angular orientations of the images selected as end-views for two-dimensional averaging, and in the different methods employed to sort the heterogeneous data set in the two approaches.

Accompanying this apical change is a partial constriction of the *trans* cavity opening, from a diameter of ~40 Å to ~30 Å. Constriction of the *trans* opening could restrict access for a second GS, and may be a structural manifestation of negative cooperativity for substrate binding between the two halves of the GroEL (Yifrach & Horovitz, 1995), consistent with the observed 1:1 binding stoichiometry of binding of many different substrates (Aoki *et al.*, 1997; Brazil *et al.*, 1998; Chen *et al.*, 1994; Lin *et al.*, 1995). Neither the apical domain repositioning nor the constriction of the

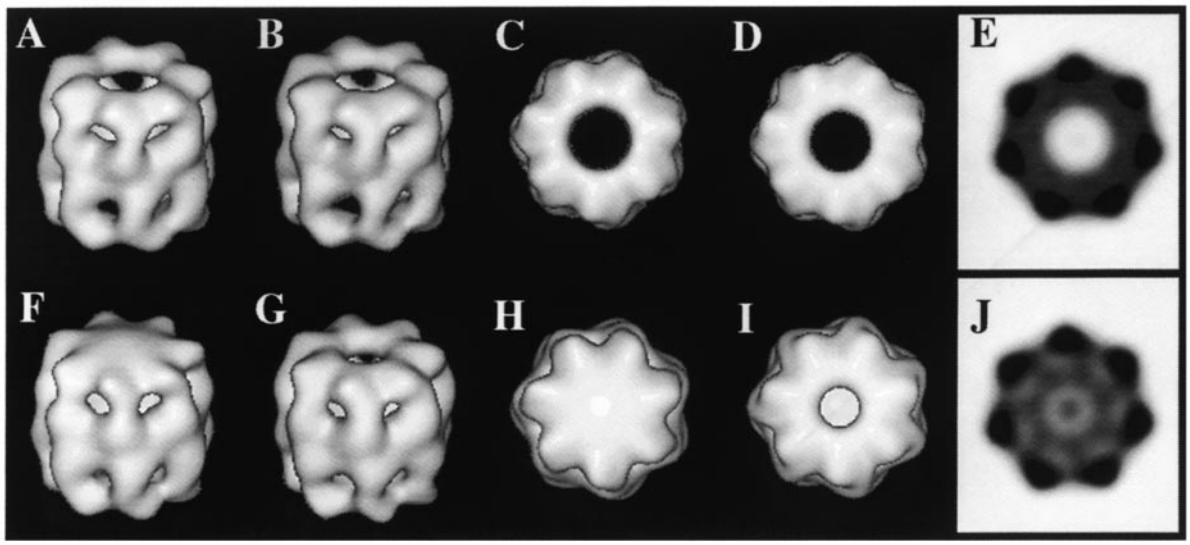

Figure 5. Three-dimensional reconstructions from cryoEM images of the GroEL-GS sample: (a)-(d), surface representations of the reconstruction of the 2999 images that correlated best with the unmodified crystal structure of GroEL; (f)-(i), reconstruction of the 1998 images that correlated to the GroEL model with a GS monomer added to one end; (e) and (j), reprojections of the two reconstructions in end-view. The surface views show both ends of each reconstruction, tilted at 30° and 90° from side-view. The first reconstruction shows no significant difference from the crystal structure, while the second has several particularly notable features: a protrusion of GS density from one end (*cis*) of the GroEL, obscuring the cavity opening, a reduction of the outer diameter of both apical domain rings, and a constriction of the *trans* cavity opening. None of these characteristics, including the partially exposed location of the GS, was incorporated in the starting model. Reprojection of the first reconstruction (e) exhibits no chirality, as expected from the almost-perfect 2-fold symmetry of the structure, while that of the second class of images (j) shows a handedness similar to, though weaker than, that seen with the averaged projection images (Figure 3(f)). All reconstructions were surfaced at 95% of the protein volume to highlight structural features.

opening is a feature of the starting model of GroEL-GS. Our three-dimensional reconstruction of the GroEL-GS complex thus reveals that the structural changes visible in two-dimensional analysis are complex and involve both the *cis* and *trans* rings. However, an unambiguous explanation of the changes taking place is difficult at the resolution of this reconstruction, and must await more detailed structural study.

As a control in our three-dimensional sorting and reconstruction protocol, a parallel sorting and reconstruction procedure was applied to images of GroEL in the absence of GS, using the same two initial models. Surprisingly, the GroEL images were initially evenly divided between the two reference models, and reconstruction and refinement were carried out for both classes. With refinement, the number of images correlating preferably to the GroEL-GS model dropped to ~10%. More importantly, the distinguishing feature of this model, the presence of the additional GS density, virtually disappeared with the first few rounds of refinement. The changes in GroEL conformation seen in the GroEL-GS structure (constriction of the apical opening, inward movement of apical domains) were not visible at any stage of reconstruction of the unliganded GroEL data, from initial to final, in reconstructions from either model.

When one compares the GroEL conformational transitions induced by GroES and/or nucleotide binding with those induced by GS, it is apparent that protein substrate-induced changes are not nearly as extensive. Conformational changes caused by nucleotide are mainly characterized by anticlockwise rotations of the apical domains, resulting in sequestration of the protein substrate-binding sites away from the cavity interior. The structural effects that accompany nucleotide and GroES binding are not limited to the apical domain regions. Significant changes also take place in the inter-ring contacts at the equatorial domains as well as a slight expansion of the cavity opening in the ring *trans* to GroES binding (Roseman *et al.*, 1996; White *et al.*, 1997). Though the detailed nature of the structural changes in GroEL elicited by binding GS are difficult to determine due to the limited resolution of this study, some differences from the nucleotide and GroES-triggered changes are apparent. In contrast to the expansion of the *trans*-opening with GroES binding, the most recognizable structural change induced by GS is a constriction of the opening to the *trans* cavity, consistent with negative cooperativity in substrate binding. The major displacement of the apical domains noted is radially inward, possibly a result of a more complex rotation, but similar in appearance to that noted in projection when GroEL-ATP complexes were subjected to elevated temperatures

(45 °C; Llorca *et al*., 1998). Our current goal is the determination of the GroEL-GS structure at higher resolution to better characterize the domain motions that result in the observed configurational changes.

In contrast to the structural studies presented here, previous electron microscopy studies involving GroEL bound to model substrates have in general used smaller proteins, or examined complexes in the presence of GroES (Braig *et al*., 1994; Chen *et al*., 1994; Langer *et al*., 1992; Sparrer *et al*., 1997). These studies have localized the substrate to the GroEL (or GroEL-GroES) cavity, but have not detected any significant alteration of the conformation of GroEL, beyond that caused by nucleotide, or by GroES in those cases where the co-chaperonin was present. The conformational changes in GroEL that we report here may simply reflect the binding of a relatively large polypeptide substrate in the absence of nucleotide or other cofactor. We suggest that a major difference between previous observations and our current one may be some physical property of the substrate protein, for example its size, which may force GroEL to undergo some degree of structural change.

Acknowledgments

This work was funded in part by a grant from the University of Missouri Research Board (E.P.G.) and from the National Institutes of Health (GM49309, M.T.F.). We thank Simon Low and Daniel Kennicutt for their technical assistance in this work.

References

Aoki, K., Taguchi, H., Shindo, Y., Yoshida, M., Ogasahara, K., Yutani, K. & Tanaka, N. (1997). Calorimetric observation of a GroEL-protein binding reaction with little contribution of hydrophobic interaction. *J. Biol. Chem.* **272**, 32158-32162.

Braig, K., Otwinowski, Z., Hegde, R., Boisvert, D. C., Joachimiak, A., Horwich, A. L. & Sigler, P. B. (1994). The crystal structure of the bacterial chaperonin GroEL at 2.8 Å. *Nature,* **371**, 578-586.

Brazil, B. T., Ybarra, J. & Horovitz, P. M. (1998). Divalent cations can induce the exposure of GroEL hydrophobic surfaces and strengthen GroEL hydrophobic binding interactions: novel effects of Zn^{2+} on GroEL interactions. *J. Biol. Chem.* **273**, 3257-3263.

Brunschier, R., Danner, M. & Seckler, R. (1993). Interactions of phase P22 tailspike protein with GroE molecular chaperones during refolding *in vitro*. *J. Biol. Chem.* **268**, 2767-2772.

Chen, S., Roseman, A. M., Hunter, A. S., Wood, S. P., Burston, S. G., Ranson, N. A., Clarke, A. R. & Saibil, H. R. (1994). Location of a folding protein and shape changes in GroEL-GroES complexes imaged by cryo-electron microscopy. *Nature,* **371**, 261-264.

Churchich, J. E. (1997). Conformational changes at the nucleotide binding of GroEL induced by binding of protein substrates. *J. Biol. Chem.* **272**, 19645-19648.

Coyle, J. E., Texter, F. L., Ashcroft, A. E., Masselos, D., Robinson, C. V. & Radford, S. E. (1999). GroEL accelerates the refolding of hen lysozyme without changing its folding mechanism. *Nature Struct. Biol.* **6**, 683-690.

Farr, G. W., Furtak, K., Rowland, M. B., Ranson, N. A., Saibil, H. R., Kirchhausen, T. & Horwich, A. L. (2000). Multivalent binding of nonnative substrate proteins by the chaperonin GroEL. *Cell,* **100**, 561-573.

Fenton, W. A. & Horwich, A. L. (1997). GroEL-mediated protein folding. *Protein Sci.* **6**, 743-760.

Fenton, W. A., Kashi, Y., Furtak, K. & Horwich, A. L. (1994). Residues in chaperonin GroEL required for polypeptide binding and release. *Nature,* **371**, 614-619.

Fisher, M. T. (1992). Promotion of the *in vitro* renaturation of dodecameric glutamine synthetase from *Escherichia coli* in the presence of GroEL (chaperonin-60) and ATP. *Biochemistry,* **31**, 3955-3963.

Fisher, M. T. (1993). On the assembly of dodecameric glutamine synthetase from stable chaperonin complexes. *J. Biol. Chem.* **269**, 13629-13636.

Fisher, M. T. (1994). The effect of GroES on the GroEL-dependent assembly of dodecameric glutamine synthetase in the presence of ATP and ADP. *J. Biol. Chem.* **260**, 13629-13636.

Frank, J., Radermacher, M., Penczek, P., Zhu, J., Li, Y., Ladjadj, M. & Leith, A. (1996). SPIDER and WEB: processing and visualizaiton of images in 3D electron microsocpy and other fields. *J. Struct. Biol.* **116**, 190-199.

Hunt, J. F., Weaver, A. J., Landry, S. J., Gierasch, L. & Diesenhofer, J. (1996). The crystal structure of the GroES chaperonin at 2.8 Å resolution. *Nature,* **379**, 37-45.

Langer, T., Pfeifer, G., Martin, J., Baumeister, W. & Hartl, F.-U. (1992). Chaperonin-mediated protein folding: GroES binds to one end of the GroEL cylinder, which accommodates the protein substrate within its central cavity. *EMBO J.* **11**, 4757-4765.

Lin, Z., Schwarz, F. P. & Eisenstein, E. (1995). The hydrophobic nature of GroEL-substrate binding. *J. Biol. Chem.* **270**, 1011-1014.

Llorca, O., Galan, A., Carrascosa, J. L., Muga, A. & Vlapuesta, J. M. (1998). GroEL under heat-shock. *J. Biol. Chem.* **273**, 32587-32594.

Llorca, O., McCormack, E. A., Hynes, G., Grantham, J., Cordell, J., Carrascosa, J. L., Willison, K. R., Fernandez, J. J. & Valpuesta, J. M. (1999). Eukaryotic type II chaperonin CCT interacts with actin through specific subunits. *Nature,* **402**, 693-696.

Mande, S. C., Mehra, V., Bloom, B. R. & Hol, W. G. J. (1996). Structure of the heat shock protein chaperonin-10 of *Mycobacterium leprae*. *Science,* **258**, 203-207.

Mendoza, J. A. & Campo, G. D. (1996). Ligand-induced conformational changes of GroEL are dependent on the bound substrate polypeptide. *J. Biol. Chem.* **271**, 16344-16349.

Penczek, P., Radermacher, M. & Frank, J. (1992). Three-dimensional reconstruction of single particles embedded in ice. *Ultramicroscopy,* **40**, 33-53.

Penczek, P. A., Zhu, J. & Frank, J. (1996). A common-lines based method for determining orientations for $N > 3$ particle projections simultaneously. *Ultramicroscopy,* **63**, 205-218.

Roseman, A. M., Chen, S., White, H., Braig, K. & Saibil, H. R. (1996). The chaperonin ATPase cycle: mechanism of allosteric switching and movements of substrate-binding domains in GroEL. *Cell*, **87**, 241-251.

Rye, H. S., Roseman, A. M., Chen, S., Furtak, K., Fenton, W., Saibil, H. & Horwich, A. L. (1999). GroEL-GroES Cycling: ATP and nonnative polypeptide direct altenation of folding-active rings. *Cell,* **97**, 325-338.

Sakikawa, C., Taguchi, H., Makino, Y. & Yoshida, M. (1999). On the maximum size of proteins to stay and fold in the cavity of GroEL underneath GroES. *J. Biol. Chem.* **274**, 21251-21256.

Schmidt, M., Buchner, J., Todd, M. J., Lorimer, G. H. & Viitanen, P. (1994). On the role of GroES in the chaperonin-assisted folding reaction. *J. Biol. Chem.* **269**, 10304-10311.

Sigler, P. B., Xu, Z., Rye, H. S., Burston, S. G., Fenton, W. A. & Horwich, A. L. (1998). Structure and function in GroEL-mediated protein folding. *Annu. Rev. Biochem.* **67**, 581-608.

Sparrer, H., Rutkat, K. & Buchner, J. (1997). Catalysis of protein folding by symmetric chaperone complexes. *Proc. Natl Acad. Sci. USA,* **94**, 1096-1100.

Thiyagarajan, P., Henderson, S. J. & Joachimiak, A. (1996). Solution structures of GroEL and its complex with rhodanese from small-angle neutron scattering. *Structure,* **4**, 79-98.

Voziyan, P. A. & Fisher, M. T. (2000). Chaperonin-assisted folding of glutamine synthetase under non-permissive conditions: off-pathway aggregation propensity does not determine the co-chaperonin requirement. *Protein Sci.* **9**, 2405-2412.

Wang, J. D. & Weissman, J. S. (1999). Thinking outside the box: new insights into the mechanism of GroEL-mediaited protein folding. *Nature Struct. Biol.* **6**, 597-600.

White, H. E., Chen, S., Roseman, A. M., Yifrach, O., Horovitz, A. & Saibil, H. (1997). Structural basis of allosteric changes in the GroEL mutant Arg197 → Ala. *Nature Struct. Biol.* **4**, 690-694.

Xu, Z. & Sigler, P. B. (1998). GroEL/GroES: structure and function of a two-stroke folding machine. *J. Struct. Biol.* **124**, 129-141.

Xu, Z., Horwich, A. L. & Sigler, P. B. (1997). The crystal structure of the asymmetric GroEL-GroES-$(ADP)_7$ chaperonin complex. *Nature,* **388**, 741-750.

Yamashita, M. M., Almassy, R. J., Janson, C. A., Cascio, D. & Eisenberg, D. (1989). Refined atomic model of glutamine synthetase at 3.5 Å resolution. *J. Biol. Chem.* **264**, 17681-17690.

Yifrach, O. & Horovitz, A. (1995). Nested cooperativity in the ATPase activity of the oligomeric chaperonin GroEL. *Biochemistry,* **34**, 5303-5308.

Yifrach, O. & Horovitz, A. (1996). Allosteric control by ATP of non-folded protein binding to GroEL. *J. Mol. Biol.* **255**, 356-361.

Edited by W. Baumeister

(Received 22 November 2000; received in revised form 15 February 2001; accepted 6 March 2001)